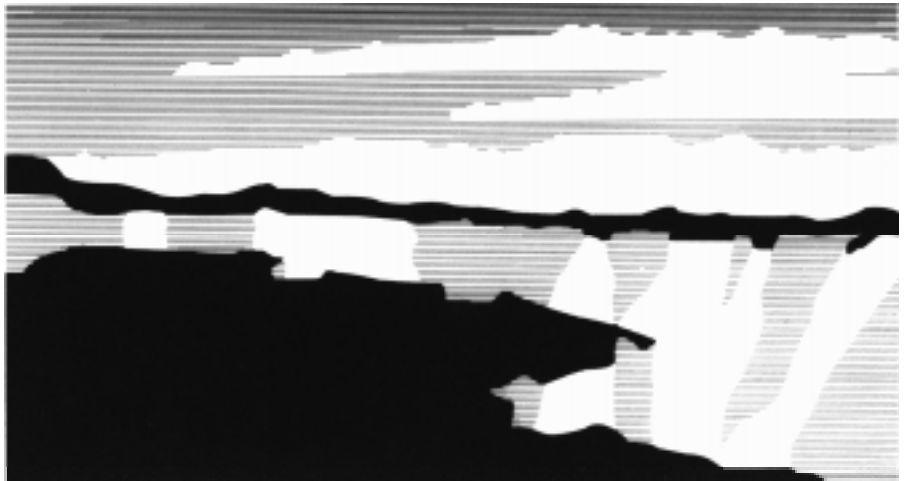


Title: **The Effect of Urban Canopy
Parameterizations on Mesoscale
Meteorological Model Simulations in the
Paseo Del Norte Area**

Author(s): Michael J. Brown & Michael D. Williams

Submitted to: Air and Waste Management Association's 90th Annual
Meeting, June 8 - 13, 1997, Toronto, Canada



Los Alamos
NATIONAL LABORATORY

Los Alamos National Laboratory, an affirmative action/equal opportunity employer, is operated by the University of California for the U.S. Department of Energy under contract W-7405-ENG-36. By acceptance of this article, the publisher recognizes that the U.S. Government retains a nonexclusive, royalty-free license to publish or reproduce the published form of this contribution, or to allow others to do so, for U.S. Government purposes. The Los Alamos National Laboratory requests that the publisher identify this article as work performed under the auspices of the U.S. Department of Energy. Los Alamos National Laboratory strongly supports academic freedom and a researcher's right to publish; therefore, the Laboratory as an institution does not endorse the viewpoint of a publication or guarantee its technical correctness.

For Presentation at the Air & Waste Management Association's 90th Annual Meeting & Exhibition, June 8-13, 1997, Toronto, Ontario, Canada

97-A1062

The effect of urban canopy parameterizations on mesoscale meteorological model simulations in the Paso del Norte area.

Michael J. Brown and Michael D. Williams

Los Alamos National Laboratory, Energy and Environmental Analysis Group,
Group TSA-4, MS F604, Los Alamos, NM 87545

Abstract

Since mesoscale numerical models do not have the spatial resolution to directly simulate the fluid dynamics and thermodynamics in and around urban structures, urban canopy parameterizations are sometimes used to approximate the drag, heating, and enhanced turbulent kinetic energy (tke) produced by the sub-grid scale urban elements. In this paper, we investigate the effect of the urban canopy parameterizations used in the HOTMAC mesoscale meteorological model by turning the parameterizations on and off. The model simulations were performed in the Paso del Norte region, which includes the cities of El Paso and Ciudad Juarez, the Franklin and Sierra Juarez mountains, and the Rio Grande. The metropolitan area is surrounded by relatively barren scrubland and strips of vegetation along the Rio Grande. Results indicate that the urban canopy parameterizations do affect the mesoscale flow field, reducing the magnitude of wind speed and changing the magnitude of the sensible heat flux and tke in the metropolitan area. A nighttime heat island and a daytime cool island exist when urban canopy parameters are turned on, but associated recirculation flows are not readily apparent. Although model-computed solar and net radiation values look reasonable, the relationship between urban and rural longwave radiation fluxes does not agree with published measurements.

Introduction

The US Environmental Protection Agency and the US Department of Energy are sponsoring a US-Mexico border air quality project in the Paso del Norte. Some of the key players in the project are EPA Region VI, Sonoma Technologies, the Mexican Petroleum Institute, the Texas Natural Resource Conservation Commission, the Environmental Defense Fund, Ciudad Juarez Department of Water and Sanitation, EPA National Exposure Research Laboratory, Environ, the Desert Research Institute, as well as Los Alamos National Laboratory (LANL). As part of this larger project, LANL is involved in studying the atmospheric circulations that develop in the region for the purpose of better understanding ozone production and transport. One area of particular focus involves assessing the importance of the urban heat island circulation on the overall wind patterns that develop due to interaction with mountain-induced flows and synoptically-driven winds. Using the HOTMAC mesoscale meteorological model, we can separate the effects of the urban canopy from the mountain-induced and synoptically-driven winds by turning the urban canopy parameterizations on and off. Although the urban canopy parameterizations are themselves approximations,

placing a minimal amount of confidence in them allows us to obtain a first-order evaluation of the importance of the urban canopy. Future research efforts include evaluating the urban canopy parameterizations by comparing model results to meteorological measurements performed during a summer 1996 intensive field campaign held in the Paso del Norte region. (1)

Background

Field experiments indicate that the mean temperature of a city center can be from 1-10 °C warmer than the surrounding rural areas during the night and anywhere from a few degrees warmer to a few degrees cooler during the daytime. (2) The nighttime warming results, in part, from the high heat capacity of building and road materials, the release of heat from combustion and other anthropogenic sources, and trapping of longwave radiation in urban canyons. (3) In calm wind conditions, the warmer central core results in a thermally-induced recirculation that is radially inward near the surface, rising upward above the city center, and radially outward at elevations aloft. (4) The buildings in an urban area result in reduced wind speeds by imparting drag onto the larger-scale flow and mechanically create turbulence due to increased surface roughness. (2)

A number of numerical modeling studies of an idealized urban heat island have been performed, where the only driver of fluid flow is the horizontal temperature gradient. (5,6) In a study more representative of an actual city, the Tokyo urban heat island was simulated in a cross-flow. (7) Although the authors ignored topography, they found reasonable agreement between measured and modeled vertical profiles of temperature. Numerous numerical modeling studies have been performed with cities situated in complex topography, but in general the urban canopy was not fully parameterized. (8,9) One 2-d simulation performed in the Los Angeles basin area found that the urban canopy effects on the mesoscale flow field are negligible when compared to the sea-breeze and mountain-induced slope flows. (10) However, in a 3-d simulation of the St. Louis area using the RAMS prognostic meteorological model, it was discovered that the urban heat island had a significant impact on the computed meteorological fields. (11) The differences between the simulations are most likely due to the steeper topography and the land/ocean interface found in the Los Angeles case, although model and urban canopy parameterization deviations might also be responsible. In all of the modeling studies cited above, it appears that urban canopy parameterizations for short- and longwave attenuation, momentum drag, and tke production were not utilized. Below, we describe how the urban canopy is accounted for in the HOTMAC meteorological model.

Model Description

HOTMAC (Higher-Order Turbulence Model for Atmospheric Circulation) is a three-dimensional time-dependent mesoscale meteorological model. (12) Using the hydrostatic approximation, a gradient-diffusion closure scheme for the horizontal turbulence components, and a terrain-following coordinate system, the governing conservation equations for mass, momentum, heat, and moisture are solved numerically using the alternating direction implicit (ADI) finite difference scheme. A simple 4-point diffusive smoothing scheme with smoothing parameter $\gamma = 0.3$ is used to remove $2 \Delta x$ waves. The vertical momentum, heat, and moisture fluxes are approximated using a one-equation $1 \frac{1}{2}$ order turbulence closure scheme, where the turbulent length scale (l) is determined from an algebraic equation and the turbulent kinetic energy (tke) is solved numerically by an ap-

proximated differential equation.

The lower boundary conditions are defined by similarity theory and a surface energy balance between short- and longwave energy and sensible, latent, and soil heat fluxes (eqn. 1). The two-stream delta-eddy method is used to solve for the incoming shortwave energy flux (13), while a prescribed surface albedo determines the outgoing shortwave flux. The upward and downward longwave radiation fluxes are determined using the Stefan-Boltzmann relation and the method of Sasamori (14), respectively. The sensible heat flux is obtained from similarity theory, while the latent heat flux is computed from a daytime-prescribed and nighttime-computed Bowen ratio. The soil heat flux is obtained by solving a 5-level heat conduction equation in the soil which ignores lateral heat transfer.

The urban canopy, too small to be resolved by the mesoscale model, has been parameterized through a) the land class descriptions, b) the short- and longwave energy flux above the ground, c) addition of an anthropogenic heating term (Q_f), d) drag in the momentum equations, and e) artificial turbulence production within the canopy. Table 1 lists the land classes and associated thermal properties used in the present simulation. In our formulation, the urban land class specification is denoted by a relatively high density, low specific heat, high thermal diffusivity, high Bowen ratio, low albedo, and low emissivity. It should be noted that these values have large uncertainty, are difficult to validate, and may vary widely within the city and from city to city. Within the HOT-MAC model, the short- and longwave radiation are forced to decay exponentially with height within the urban canopy. An anthropogenic heating term is added to the temperature equations below the canopy height, but it has not been added to the surface radiation balance (eqn 1). Finally, momentum loss and turbulence production within the urban canopy are approximated using drag coefficient (C_d) terms applied to the momentum and turbulence prognostic equations, similar to work done on forest canopies. (15)

Problem Description

The meteorological simulation was performed using a double-nested mesh composed of 13 x 16, 26 x 29, and 20 x 23 grids of size 18, 6, and 2 km, respectively (fig. 1). Sixteen vertical grid levels were used, with the vertical grid spacing (in terrain-following coordinates) being 4 m for the lowest four cells and expanding to a maximum of 700 m at the model domain top. The domain extends 4000 m above ground level (agl) in terrain-following coordinates and 6826 m above sea level (asl) in cartesian coordinates. The outermost mesh is dominated in the northern-half by the Black Range on the west, the Sacramento Mountains to the east, and San Andres Mountains in between. The topography is primarily scrubland, except on the higher mountains where mountain vegetation is the predominant landclass. The Rio Grande river valley becomes apparent on the intermediate mesh, as well as the El Paso/Ciudad Juarez metropolitan area. On the fine mesh, one can see that the Rio Grande river valley runs between the Franklin Mountains to the north and Sierra Juarez Mountains to the south and separates El Paso, Texas from Ciudad Juarez, Mexico. The thermal characteristics of the landclasses depicted in fig. 1 are given in Table 1.

The meteorological simulations were started at 6:00 pm on Sep. 9, 1994 and run for approximately thirty hours. The initial conditions for the simulations were obtained from the local airport rawinsonde sounding. A data assimilation scheme using the rawinsonde data taken at 12 hour intervals

was used to "nudge" the winds *above* 2500 meters agl. The synoptic conditions during this time period are characterized by a high pressure system over the region with northerly upper-level winds of 3-5 m/s switching to southwesterly by the end of the simulation.

Two cases were simulated, one in which the urban areas were given an urban landclass identity and the other a vegetation-scrubland landclass identity:

- Case 1: urban areas = urban landclass, $Q_f = 20$ watts/m²
- Case 2: urban areas = vegetation/scrubland landclass, $Q_f = 0$ watts/m²

Results and Discussion

Temperature Fields. Figure 2 illustrates the effect of the urban canopy on the diurnal temperature pattern at two different heights. The ground-level potential temperature (θ) computed at an urban (Sunland Park) and rural site (Turf Road, scrubland landclass) for Case 1 shows that ($\Delta\theta = \theta_{\max} - \theta_{\min}$) is smaller at the urban site. This is due primarily to larger nighttime temperatures, i.e., cooling of the urban area at night occurs at a slower rate relative to the scrubland region. At 2 m, $\Delta\theta$ at the urban site is about 10 K, close to the 12 K value measured at Sunland Park during the Sept. 1994 Border Air Quality Study. (16) Figures 3a and 4a depict the surface temperatures computed on the innermost gridmesh at 6:00 am and 2:00 pm, respectively. At 6:00 am, the urban areas are from 2-5 K warmer than the rural scrubland sites, which falls within the range measured for an ambient ten meter wind speed of roughly 3 m/s. (2) The vegetative regions that line the Rio Grande River valley have temperatures that are 5-10 K cooler than the urban area. In the afternoon, the urban landclasses are clearly cooler than the surrounding scrubland regions. This urban "cool" island phenomenon has been observed previously in several cities. (17) Comparing the above results to surface temperatures computed with urban replaced by scrubland landclass (Case 2), we find that the scrubland region along the Rio Grande river valley is quite warm relative to the surrounding areas at 6:00 am (fig. 3b). Why this occurs is not clear. Without the urban thermal properties, the urban cool island has dissappeared in the afternoon (fig. 4b).

Surface Radiation Budget. Figure 5 shows the surface energy budget computed at the urban and rural sites for Case 1, along with solar radiation data collected at the Sunland Park site during the Border Air Quality Study. (16) Four major features stand out: the total incoming solar radiation flux $S\downarrow$ is approximately the same over urban and rural sites and agrees quite well with the data; the magnitude of the outgoing solar radiation flux $S\uparrow$ is smaller at the urban site as found in prior field studies; the magnitudes of the upward and downward longwave fluxes are largest for the rural site, opposite of what is frequently measured; and the net radiation Q^* is nearly the same for the urban and rural sites in agreement with field measurements. (17) The anomalous relationship between model-computed rural and urban *upward* longwave radiation might be attributable to both a low model-prescribed emissivity (0.90 versus 0.95 suggested by ref. (17)) and the modeling assumption that only the non-building fraction of the urban canopy contributes to the upward longwave radiation flux at the surface. The anomalous relationship between urban and rural *downward* longwave radiation might be caused by uncertainty in the extinction coefficient, the value of the downward longwave radiation at canopy top, and not accounting for warming due to urban air pollution. Urban-rural longwave anomalies might also stem from a) the fact that the rural area is char-

acterized by a relatively dry and barren landscape with high thermal admittance and b) whether or not measurements of longwave fluxes are taken at canopy top or the surface.

Figure 6 depicts the net incoming shortwave radiation $S^* = S\downarrow + S\uparrow$ on the innermost grid mesh. S^* is about 20 watts/m² less over the metropolitan area for Case 1. The net shortwave radiation includes the effect of landclass albedo and attenuation by the urban canopy. The smaller albedo for the urban canopy (see Table 1) is offset by the attenuation of the incoming shortwave radiation and the smaller optical depth computed over the urban landclass, resulting in smaller S^* values over the metropolitan area for Case 1. The soil heat flux at 2:00 pm shows similar patterns for both Case 1 and 2 (fig. 7). The heat flux into the soil in the urban area is very similar to that in the scrubland regions (fig. 7a).

The *upward* longwave energy flux at 6:00 am is shown in fig. 8. Although the urban site is warmer than the rural site at night, less longwave energy is emitted upwards in the urban area according to the model (fig. 8a). The latter disagrees with most measurements and as mentioned above probably results because of a low model-prescribed emissivity and the modeling assumption that only the non-building fraction of the urban canopy contributes to the upward longwave radiation flux at the surface. The *downward* longwave energy flux at 6:00 am is shown in fig. 9. The downward longwave energy flux is smaller at the surface in the urban canopy due to longwave attenuation by the building elements (fig. 9a). The anomalies in the upward and downward longwave fluxes cancel, so that the net radiation is consistent with measurements. (17)

There is a noticeable difference in the *nighttime* sensible heat flux computed over the metropolitan area with and without the urban canopy (fig. 10). The heat flux is larger over the urban canopy due to the production, anthropogenic heating, and the release of heat within the canopy during the night. Large negative values are found at the interface between the scrubland of the Franklin Mountains and the river valley vegetation to the west. This probably occurs due to advection of warmer drainage air over the cooler air in the river valley (see fig. 3). Figure 11 shows the *daytime* sensible heat flux for Case 1 and 2. The sensible heat flux is slightly smaller over the urban canopy than in the surrounding scrubland for Case 1 (fig. 11a) and is mostly likely explained by slightly cooler temperatures and weaker turbulence over the urban canopy. The relatively large sensible heat flux over the river valley vegetation is somewhat unexpected, as the temperatures are cooler and the Bowen ratio (H_s/LE) is smaller.

Wind and Turbulence Fields. Wind vector fields computed at ten meters on the innermost grid-mesh are depicted in figs. 12 and 13. Mountain-induced upslope flows are the predominant mesoscale forcing mechanism in the afternoon for both Cases 1 and 2, respectively (figs. 12a and b). The winds are slightly smaller over the city region for the urban canopy Case 1. A few hours after sunset, the winds have reversed direction on the mountains (fig. 13). Winds are clearly much smaller over the city region for Case 1, showing that the urban canopy drag parameterizations are having an effect and in qualitative agreement with measurements. (2)

Figures 14 and 15 show the turbulent kinetic energy computed at ten meters on the innermost grid-mesh. In the afternoon, the tke over the metropolitan area is smaller when the urban canopy is turned on (fig. 14). The smaller tke values may result from the drag reduced winds and smaller sensible heat flux. Measurements suggest, however, that the tke should increase relative to back-

ground at the canopy height, but this is for a given prevailing wind speed. During the evening, the tke is significantly larger over the metropolitan area for Case 1 (fig. 15). This most likely results from the stronger wind shear and larger sensible heat flux when the urban canopy parameterizations are turned on.

Conclusions

Based solely on prognostic mesoscale meteorological model results, the urban canopy of El Paso and Ciudad Juarez does have an impact on the flow patterns that develop in the region. Relative to simulations performed with the urban landclass replaced by a scrubland landclass, the winds over the metropolitan region were generally smaller and the tke and sensible heat flux were larger during the night and smaller during the day. The surface potential temperatures showed a distinctive urban heat island during the night with intensity of 2-5 K. During the day, a cool island existed at the surface. Magnitudes of surface radiation budget terms were, in general, of similar magnitude to reported measurements. However, the magnitudes of the urban upward and downward longwave radiation fluxes were smaller than the rural values, opposite of what has been reported in the literature. This may be due to incorrect longwave flux urban canopy parameterizations, the rural area being scrubland, and/or differences in terminology. Future work involves comparison of model results to field measurements performed in the summer of 1996 (1), evaluation of longwave radiation parameterizations, and sensitivity tests of emissivity, attenuation, and anthropogenic heat flux input parameters.

References

- 1 .Roberts, P., D. Coe, T. Dye, S. Ray, and M. Arthur: Summary of measurements obtained during the 1996 Paso del Norte ozone study, final report, STI-996191-1603-FR, 1996.
- 2 .Bornstein, R.: *Mean diurnal circulation and thermodynamic evolution of urban boundary layers*, from Modeling the Urban Boundary Layer, Am. Met. Soc., Boston, MA, pp 52-94, 1987.
- 3 .Oke, T.: Boundary Layer Climates, Meuthen & Co., New York, NY, 1987.
- 4 . Arya, S.: Introduction to Micrometeorology, Academic Press, New York, NY, 1988.
- 5 .Myrup, L.: *A numerical model of the urban heat island*, J. Appl. Meteor., 8, pp 896-907, 1969.
- 6 .Venkatram, A. and R. Viskanta: *Radiative effects of elevated polluted layers*, J. Appl. Meteor., 16, pp 1256-1272, 1977.
- 7 .Saitoh T., T. Shimada, and H. Hoshi: *Modeling and simulation of the Tokyo urban heat island*, At. Env., 30, pp 3431-3442, 1996.
- 8 .Nichols, M., R. Pielke, J. Eastman, C. Finley, W. Lyons, C. Tremback, R. Walko, and W. Cotton: *Applications of the RAMS numerical model to dispersion over urban areas*, Wind Clim. Cities, pp 703-722, 1995.
- 9 .Kunz, R. and N. Moussiopolous: *Simulation of the wind field in Athens using refined boundary conditions*, At. Env., 29, pp 3575-3591, 1995.
- 10 .Schultz, P. and T. Warner: *Characteristics of summertime circulations and pollutant ventila-*

tion in the Los Angeles basin, J. Appl. Meteor., 21, pp 672-682, 1982.

- 11 .Hjelmfelt, M.: *Numerical simulation of the effects of St. Louis in mesoscale boundary-layer airflow and vertical air motion: simulations of urban vs. non-urban effects*, J. Appl. Meteor., 21, pp 1239-1257, 1982.
- 12 .Yamada, T. and S. Bunker: *A numerical model study of nocturnal drainage flows with strong wind and temperature gradients*, J. Appl. Meteor., 28, pp 545-554, 1989.
- 13 .Smith W. and C. Kao: *Numerical simulations of observed Arctic stratus clouds using a second-order turbulence closure model*, J. Appl. Meteor., 35, pp 47-59, 1996.
- 14 .Sasamori, T.: *The radiative cooling calculation for application to general circulation experiments*, J. Appl. Meteor., 7, pp 721-729, 1968.
- 15 .Yamada, T.: *A numerical study of turbulent airflow in and above a forest canopy*, J. Met.

Table 1. Landclass thermal properties used in the HOTMAC model.

	(1) VEGETATION	(2) BARE SOIL	(3) DARK SOIL	(4) ROCK(BASALT)	(5) URBAN	(6) SCRUBLAND	(7) WATER	(12) MTN. VEGETATION	(13) ROCK AND VEGETATION
BOWEN RATIO	0.5	2.0	0.5	1.5	1.5	2.5	0.1	0.5	1.0
ALBEDO	.2	.18	.12	.11	.10	.16	.10	.10	.13
EMISSIVITY	.97	.95	.98	.97	.90	.90	.99	.98	.98
SPECIFIC HEAT (J/KG/K)	3600.	1090.	1500.	753.	880.	1800.	4186.	3000.	2500.
DENSITY (KG/M^3)	1100.	1700.	2000.	2700.	2300.	1500.	1000.	1300.	1400.
THERMAL DIFFUSIVITY (M^2/S)	0.12 e-06	0.3 e-06	0.7 e-06	0.8 e-06	1.2 e-06	0.5 e-06	0.15 e-06	0.12 e-06	0.8 e-06

Equation 1. Surface energy balance at surface.

$$Q_* = R_s \downarrow + R_s \uparrow + R_L \downarrow + R_L \uparrow = H_s + LE + G_s$$

where

$$Q_* = \text{net radiation}$$

$$R_s \downarrow = \text{downward shortwave radiation}$$

$$R_s \uparrow = \text{upward shortwave radiation} = R_s \downarrow (1 - \alpha)$$

$$R_L \downarrow = \text{downward longwave radiation}$$

$$R_L \uparrow = \text{upward longwave radiation} = \varepsilon \sigma T_G^4 + (1 - \varepsilon) R_L \downarrow$$

$$H_s = \text{sensible heat flux} \approx -\rho c_p u_* T_*$$

$$LE = \text{latent heat flux} = H_s / B$$

$$G_s = \text{soil heat flux} = K_s \partial T_s / \partial z_s$$

and α is the albedo, ε is the emissivity, σ is the Stefan-Boltzman constant, T_G is the ground temperature, ρ is the air density, c_p is specific heat, u_* is the friction velocity, T_* is the temperature scale, B is the Bowen ratio, and K_s is the thermal diffusivity of the soil.

Figure 1. The three computational grid meshes with topography and landclass. The landclass key is: (1) - vegetation, (2) - bare soil, (3) - dark soil, (4) - rock (basalt), (5) - urban, (6) - scrubland, and (7) - mountain vegetation. The utm coordinates for the SW corners of the coarse, intermediate, and fine meshes are (338, 3498), (266, 3468) and (230, 3450) kilometers, respectively.

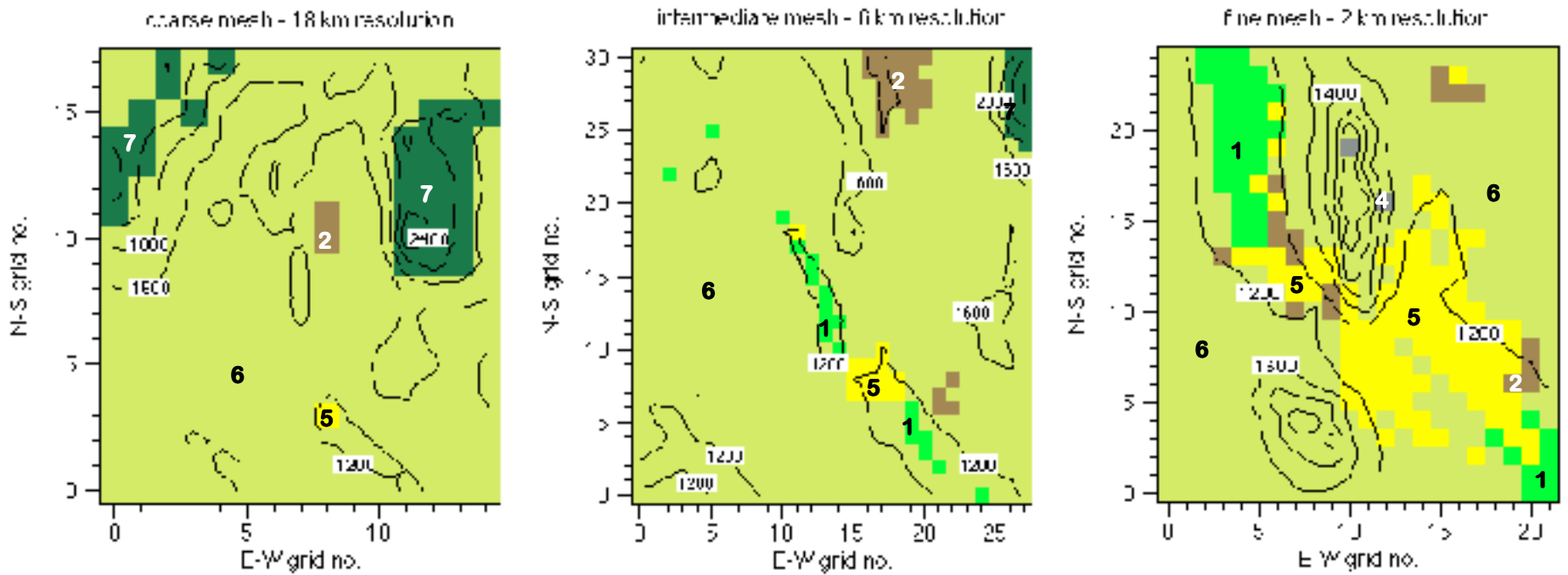


Figure 2. The ground-level and 2 meter potential temperature computed at the urban (Sunland Park) and rural (Turf Road) sites on Sept. 10, 1994. Notice that the urban site is always warmer than the rural site at 2m agl, but that the rural site is warmer in the afternoon at ground-level. Simulation start time at 6 pm on Sept. 9.

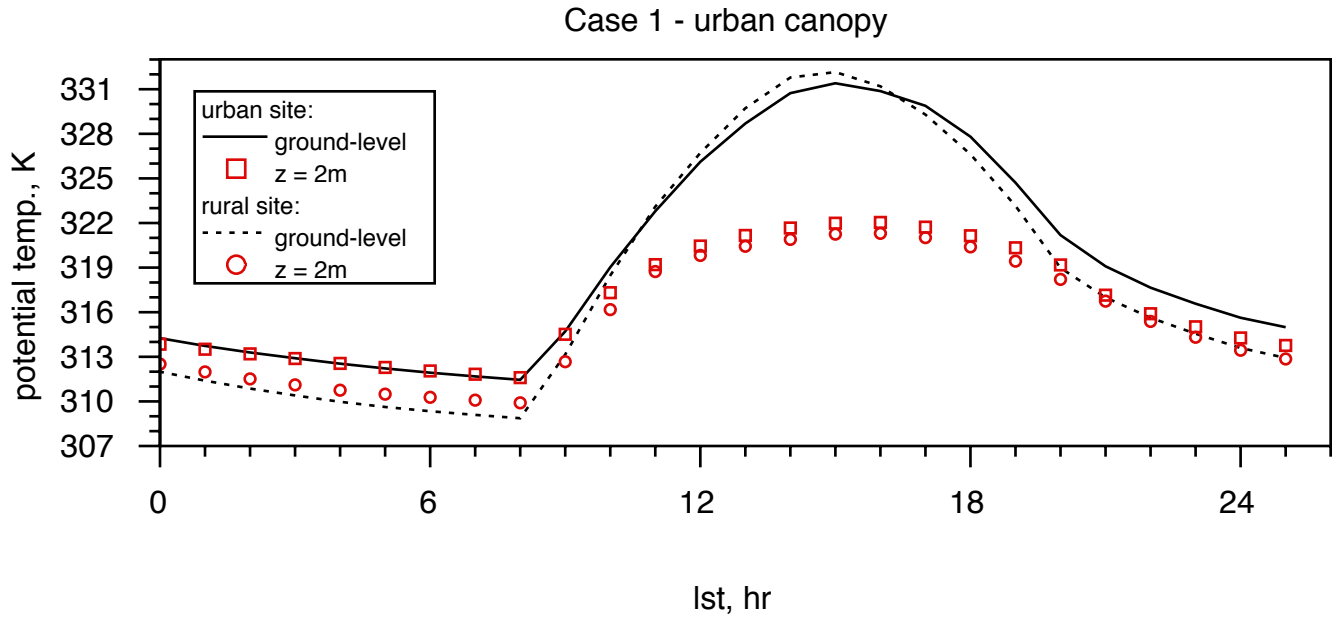


Figure 3. The ground-level potential temperature fields computed at 6:00 am for a) Case 1 and b) Case 2. For Case 1, the metropolitan areas are represented by the urban landclass, while for Case 2 by scrubland landclass. Surprisingly, for Case 2 the scrubland region in the metropolitan region remains quite warm during the night. The metropolitan area is outlined in white. S, A, and T are the Sunland Park, Airport, and Turf Road sites, respectively.

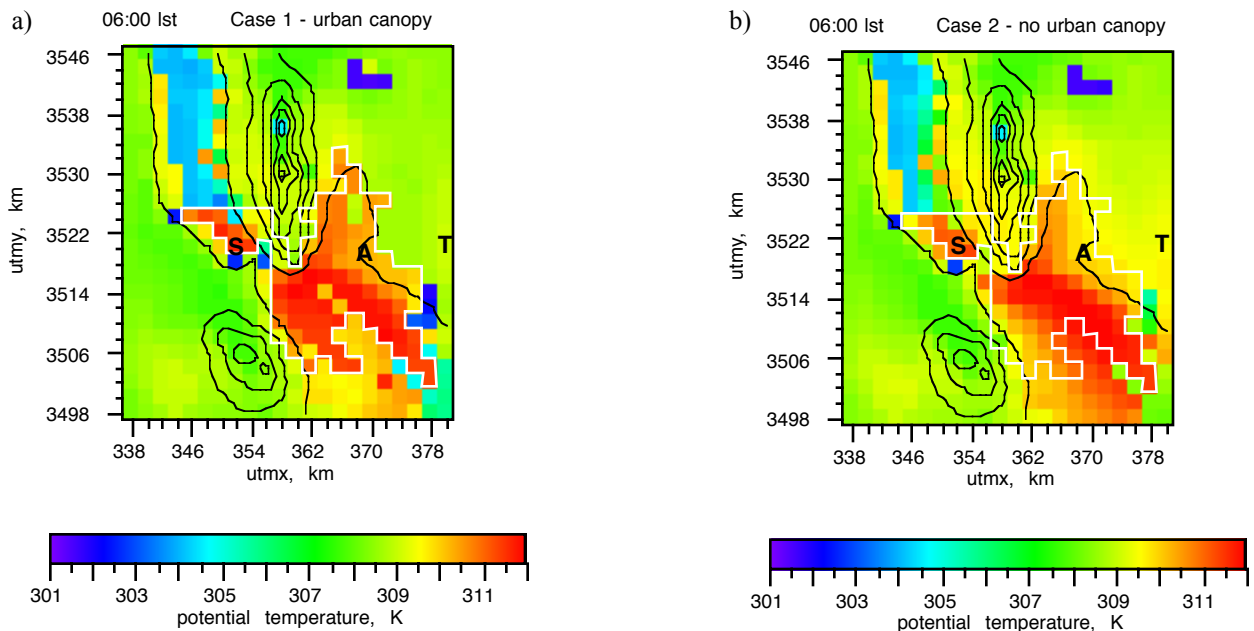


Figure 4. The ground-level potential temperature fields computed at 2:00 pm for a) Case 1 and b) Case 2. For Case 1, an urban “cool” island is apparent (however, at 2 meters agl, the “cool” island disappears).

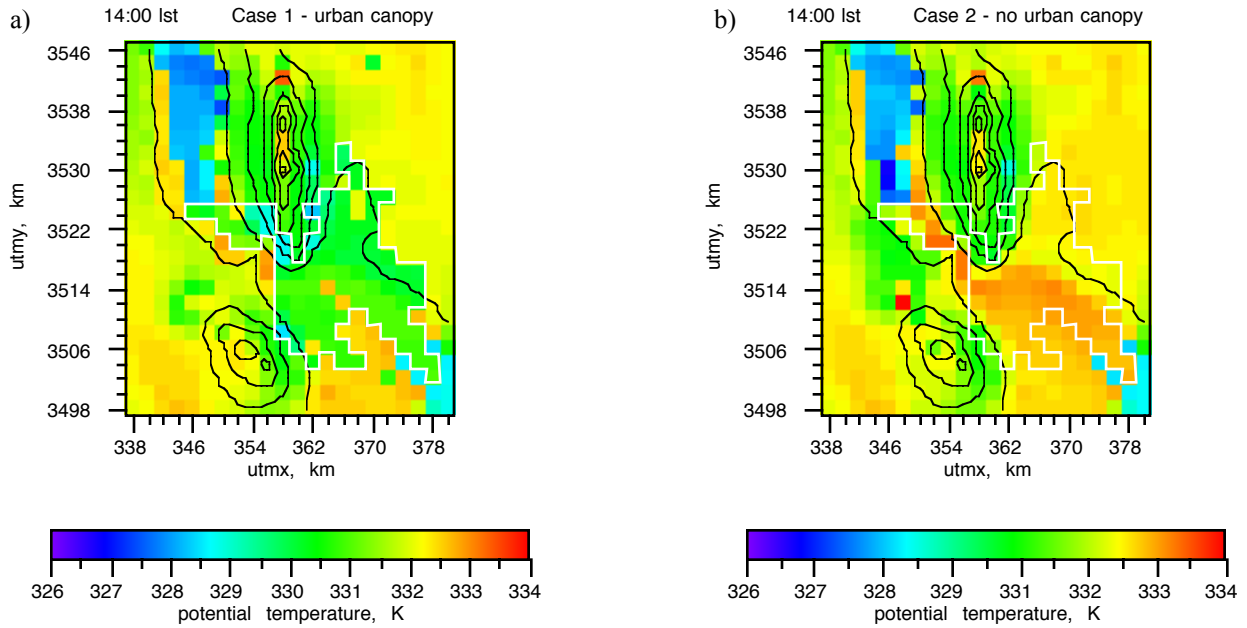


Figure 5. Diurnal variation of the computed surface energy budget terms at the urban (Sunland Park) and rural (Turf Road) sites on Sept. 10, 1994. Incoming solar radiation measurements are from the Border Air Quality Study. (17) Note that S_{\downarrow} , L_{\downarrow} , and L_{\uparrow} are computed at the top of the urban canopy.

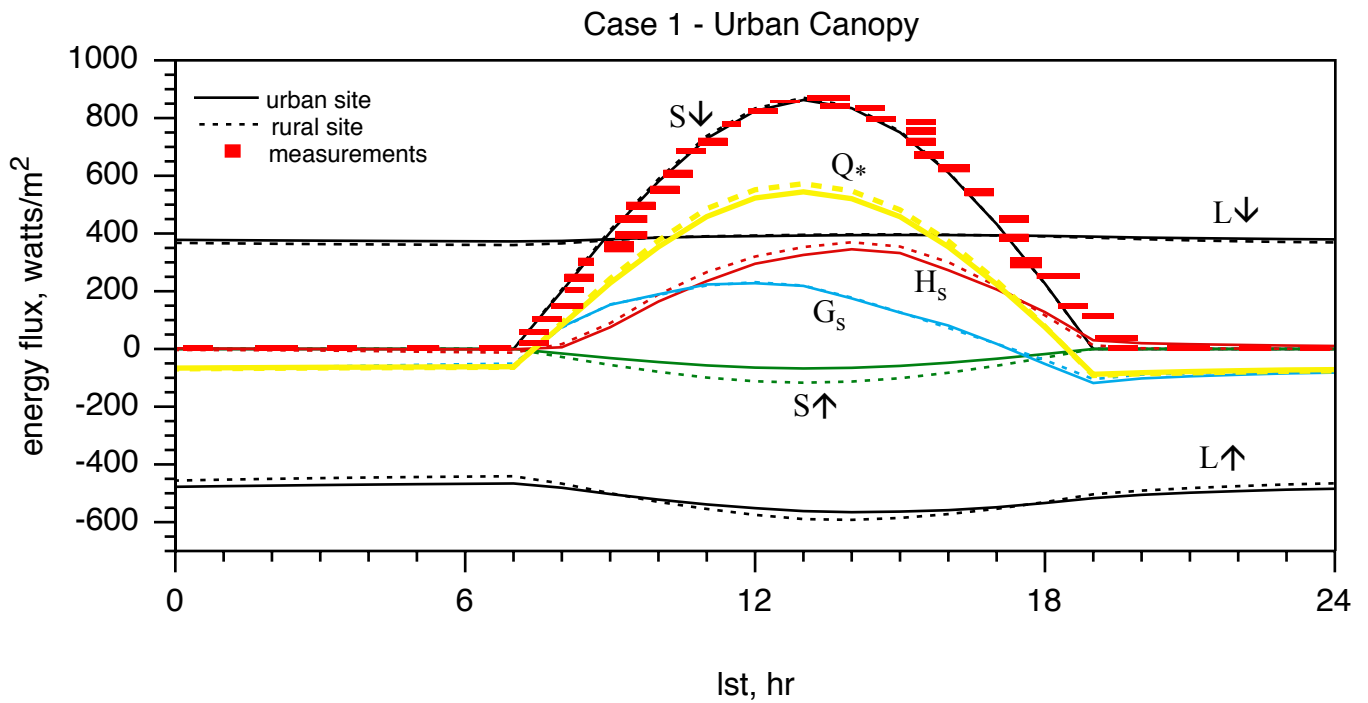


Figure 6. The net incoming shortwave computed at 2:00 pm for a) Case 1 and b) Case 2. The net shortwave includes the effect of albedo and attenuation by urban canopy elements. A shortwave deficit is found over the urban area for Case 1.

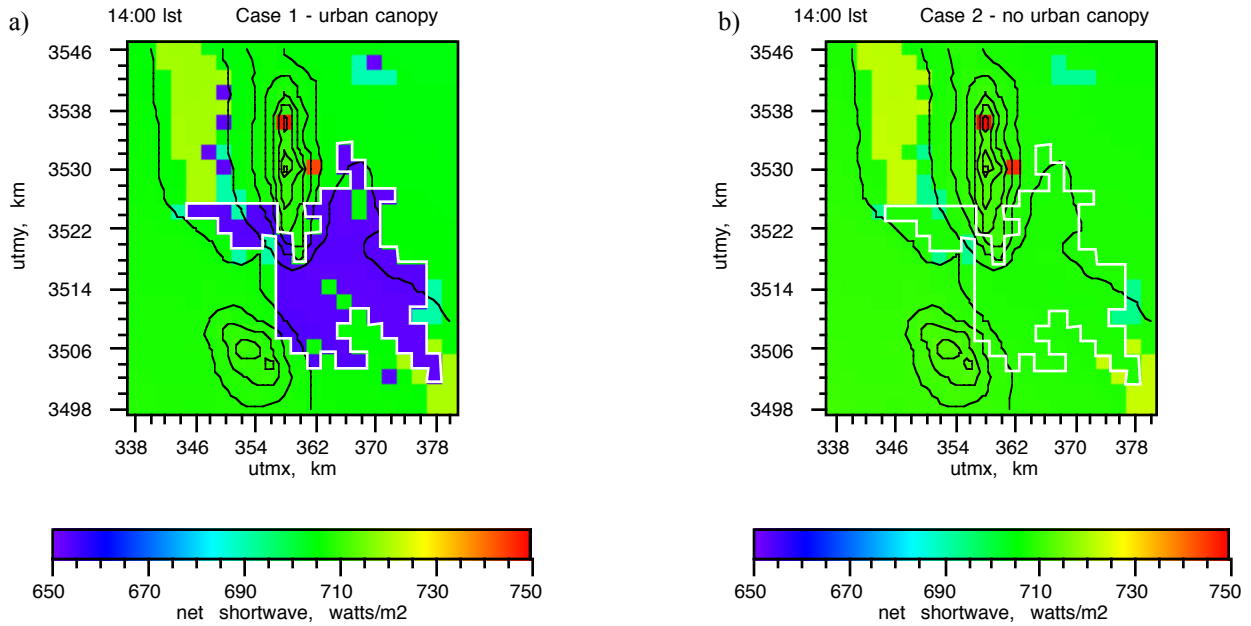


Figure 7. The soil heat flux computed at 2:00 pm for a) Case 1 and b) Case 2. Results are similar for both cases. An interesting variation in soil heat flux intensity is occurring to the northwest of the Sierra Juarez Mountains paralleling the surface potential temperature variation (see fig. 4).

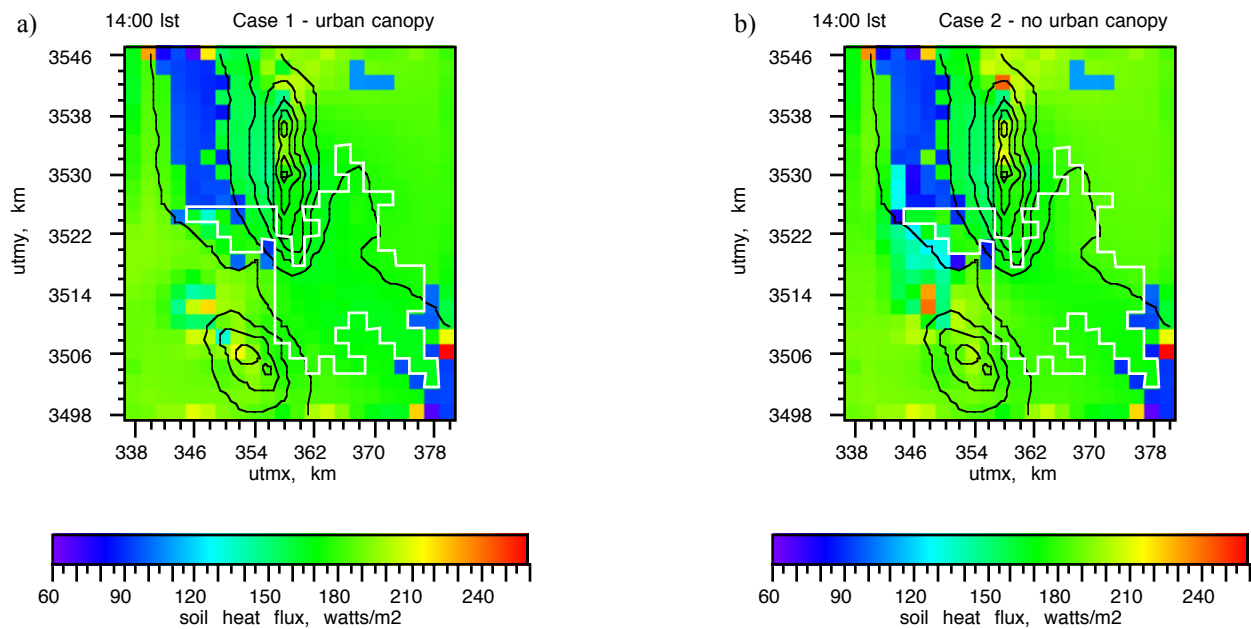


Figure 8. The canopy-top downward longwave energy flux computed at 6:00 am for a) Case 1 and b) Case 2. The magnitude of the flux for Case 2 is largest in the valley where the air temperatures are warmer. For case 1, the effect of the warmer urban canopy on the flux magnitude is apparent, though not pronounced due to the competing factor of air temperature variation with height.

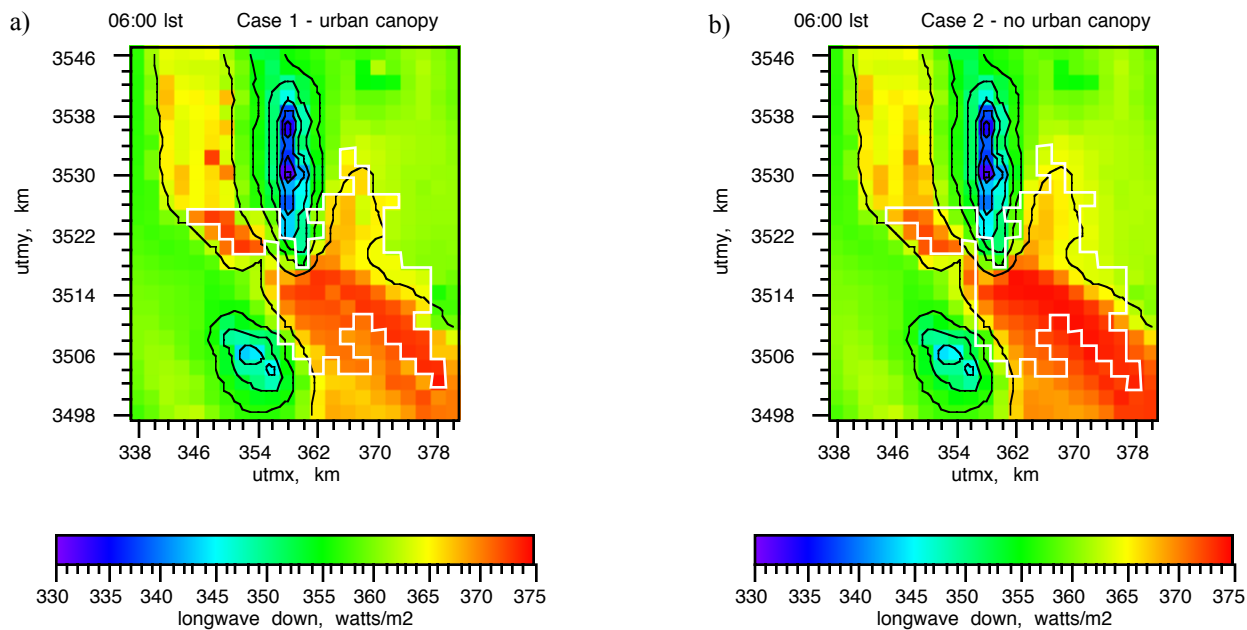


Figure 9. The canopy-top downward longwave energy flux computed at 2:00 pm for a) Case 1 and b) Case 2. The effect of the urban canopy parameterization is clear in Case 1, where the cooler temperatures over the metropolitan area result in smaller L_{\downarrow} values.

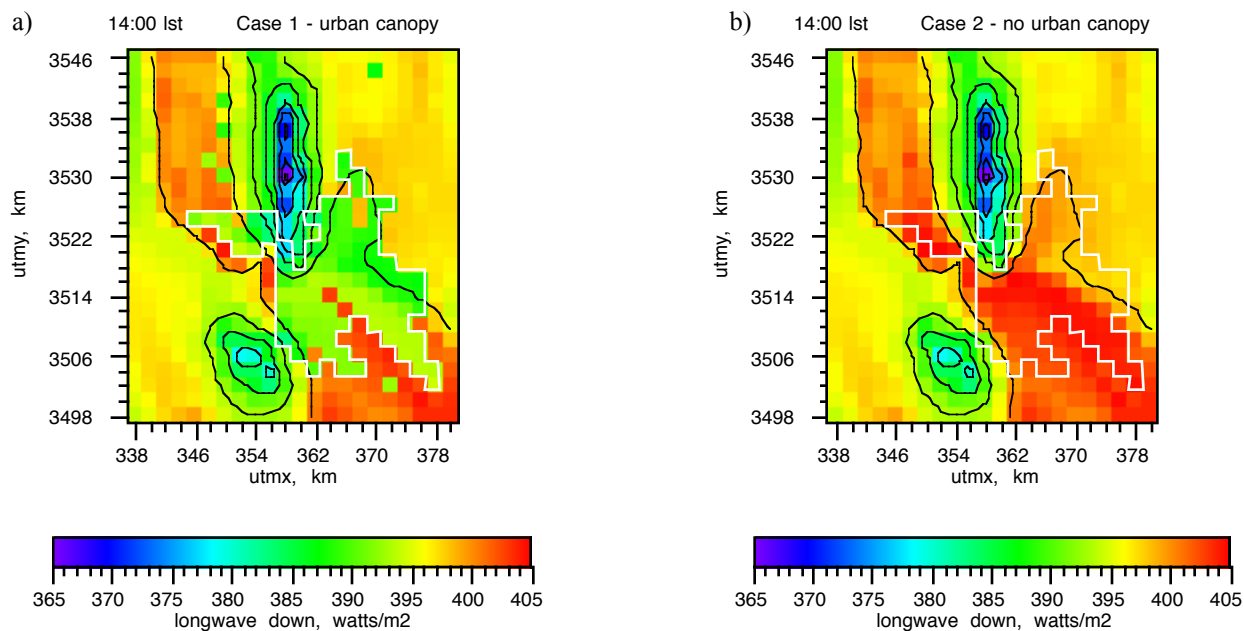


Figure 10. The sensible heat flux computed at 6:00 am for a) Case 1 and b) Case 2. The model-computed heat flux is larger over the metropolitan area when the urban canopy is present (Case 1). This is most likely due to warmer surface temperatures and stronger turbulence in the urban canopy relative to the rural scrubland during the nighttime (see figs. 3 and 13, respectively).

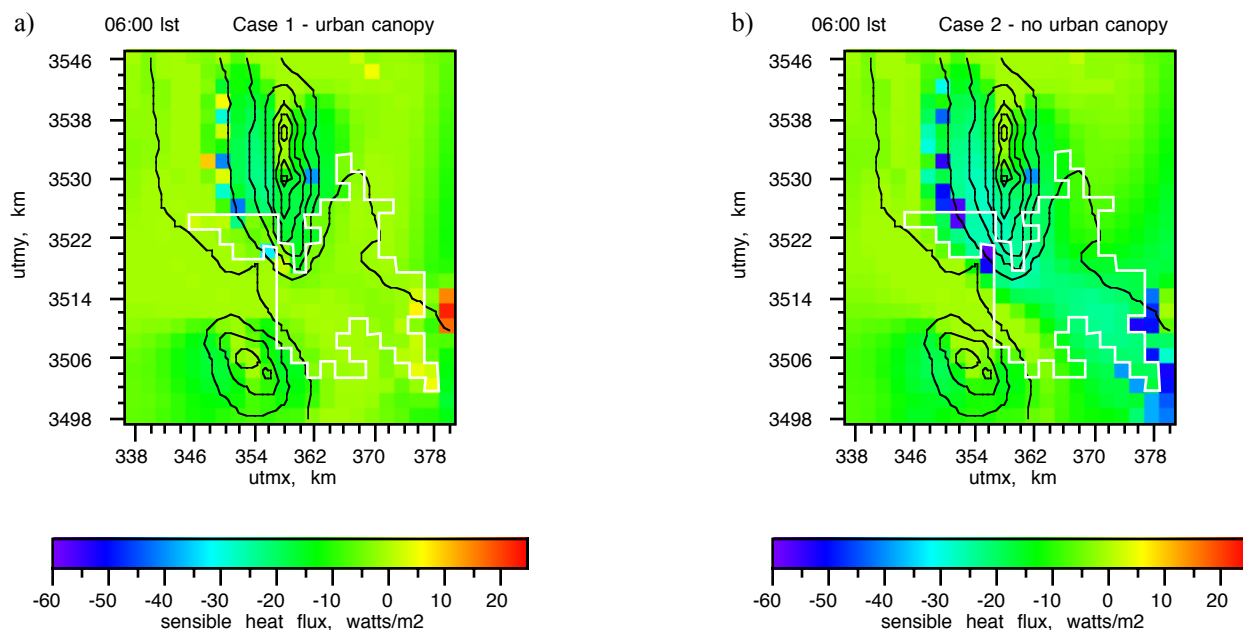


Figure 11. The sensible heat flux computed at 2:00 pm for a) Case 1 and b) Case 2. The model-computed heat flux is smaller over the metropolitan area when the urban canopy is present (Case 1). This is most likely due to cooler surface temperatures and weaker turbulence in the urban canopy relative to the rural scrubland during the daytime (see figs. 4 and 13, respectively).

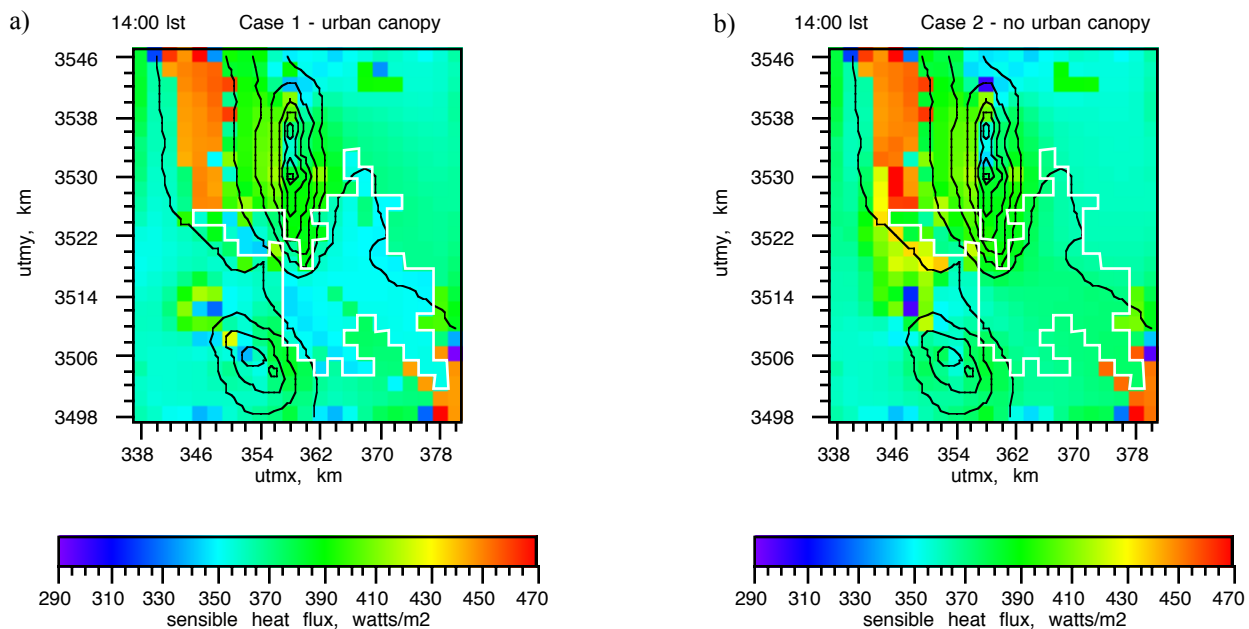


Figure 14. The turbulent kinetic energy computed at 2:00 pm for a) Case 1 and b) Case 2 at ten meters. The model-computed tke is smaller over the metropolitan area when the urban canopy is present (Case 1) resulting from the smaller winds in that region (see fig. 12).

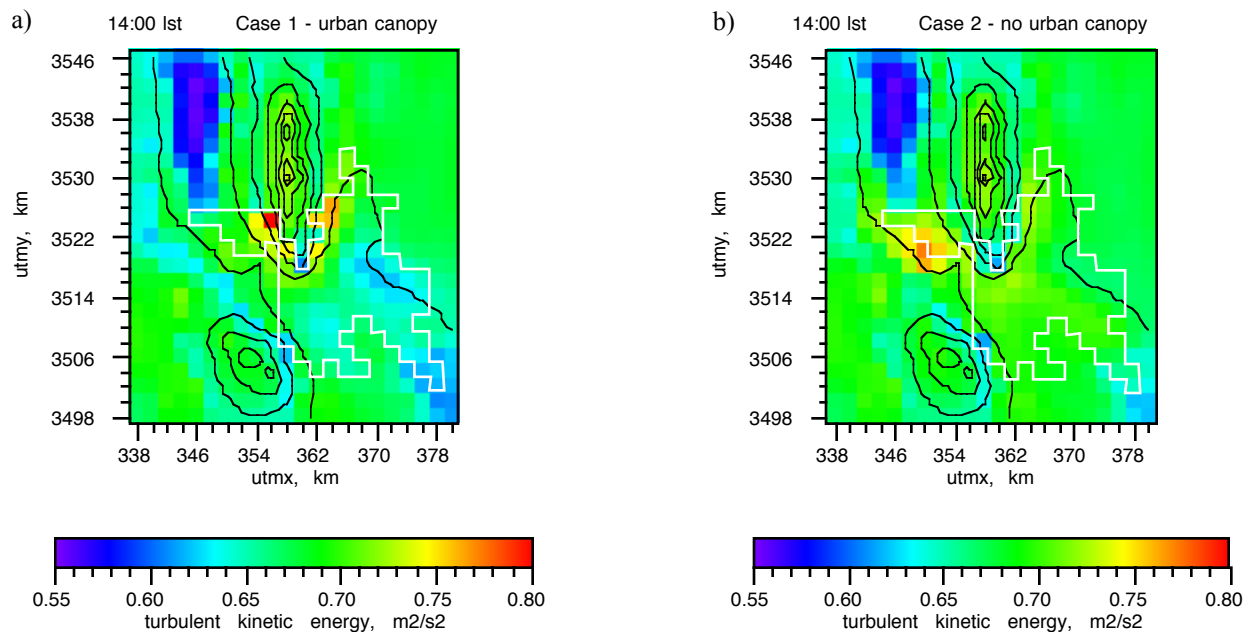


Figure 15. The turbulent kinetic energy computed at 9:00 pm for a) Case 1 and b) Case 2 at ten meters. The model-computed tke is significantly larger over the metropolitan area when the urban canopy is present (Case 1).

